



## Enhanced morphological and optoelectronic properties of organic solar cells incorporating CuO, ZnO and Au nanoparticles

Aruna P. Wanninayake<sup>1</sup> and Nidal Abu-Zahra<sup>2\*</sup>

<sup>1</sup>Department of Physics, University of Kelaniya, Kelaniya, Sri Lanka

<sup>2</sup>Materials Science and Engineering Department, University of Wisconsin-Milwaukee,  
3200 North Cramer Street, Milwaukee, WI 53201, USA

Received 13 July 2020,  
Revised 21 Nov 2020,  
Accepted 24 Nov 2020

### Keywords

- ✓ Nanoparticles;
- ✓ Semiconductor;
- ✓ EQE;
- ✓ UV-visible spectroscopy;
- ✓ PSCs

Nidal Abu-Zahra  
[nidal@uwm.edu](mailto:nidal@uwm.edu)  
+1 414 229 2668

### Abstract

The inherent electronic properties of inorganic nanoparticles; such as CuO, ZnO, and Au, make them attractive candidates to improve the performance of organic photovoltaic devices when incorporated in the active polymer layer. The incorporation of CuO nanoparticles in P3HT/PC70BM solar cells at an optimum concentration yielded a 24% improvement in the power conversion efficiency. Furthermore, the addition of Au NPs to the PEDOT:PSS layer of solar cells containing 0.6mg of CuO-NPs in the active layer increased the power conversion efficiency by 18% compared to a reference cell. However, the localized surface plasmonic resonance (LSPR) effect was not distributed into the active layer thus the light absorption in the active layer was minimized. In addition, the use of an electron transporting ZnO nanoparticles (Zn-NPs) in a buffer layer located over the active layer of P3HT/PCBM incorporating a fixed amount of CuO nanoparticles increased the power conversion efficiency by 32.19% compared to a reference cell without ZnO-NPs buffer layer.

### 1. Introduction

Bulk heterojunction (BHJ) polymer solar cells (PSCs) which are based on conjugated polymer donor and fullerene derivative acceptor materials have attracted much attention due to the efficient charge transfer from conjugated polymers to fullerene derivatives [1-5]. Organic solar cells (PSCs) usually have one important hindrance for the PCE improvement with insufficient light absorption due to the thin active layer which is restricted by the short exciton diffusion length and low carrier mobility. Therefore, efficient sun energy harvesting requires the compounds to absorb strongly in the visible region of the spectrum [6-11]. In order to enhance the optical properties of the organic thin films, many researchers have tested the metallic and metal oxide nanostructures within the thin films [12-17]. Among these compounds, nanoparticles of CuO, Au and ZnO exhibit promising inherit optoelectronic properties which can be applied to enhance the efficiency of organic solar cell devices.

Bulk CuO is considered to be an intrinsically p-type semiconductor due to copper vacancies acting as acceptors for the hole conduction. The band gap energy of CuO is 1.5 eV, which is close to the ideal energy gap of 1.4 eV required for solar cells to allow good solar spectral absorption [18-21]. Illuminated metallic nanoparticles (NPs) such as Au and other metallic nanostructures can be used to enhance the light absorption of the polymer thin films due to the localized surface plasmon resonance (LSPR) effect which contributes to a remarkable enhancement of local electromagnetic fields. Hence, this effect improves the light absorption properties of the nanostructure solar cells. Furthermore, metallic

nanostructures in the active layer can scatter the incident photons through a long propagation path resulting in a higher light absorption and photocurrent generation of PSCs [22-27]. Zinc Oxide (ZnO) is another attractive material for short-wavelength optoelectronic applications due to its wide energy band gap of 3.37 eV, large bond strength, and large exciton binding energy (60 meV) at room temperature [28]. Also, ZnO is economically cheap and an environmentally friendly n-type semiconductor which has high electron mobility, even when measured on films consisting of assembled ZnO nanoparticles [29, 30]. The combined effect of these candidates in organic solar cells improves the exciton generation, light scattering, and high charge mobility in these devices.

In this study, we present the effect of incorporating CuO NPs and Au NPs into the P3HT/PCBM (poly(3-hexylthiophene)/[6, 6]-phenyl-C70-butyric acid methyl ester) and PEDOT:PSS layers; respectively. In addition, the effect of adding a ZnO NPs buffer layer on top of the active P3HT/PCBM layer is investigated. The morphological and optoelectronic properties of the organic solar cell devices are comparatively analyzed by UV-Vis, XRD, DSC, AFM, External Quantum Efficiency (EQE) and solar simulation. Therefore, this work contributes to the understanding of the uses of CuO, Au and ZnO NPs in enhancing PSC performances.

## 2. Material and Methods

### 2.1. Materials

Three different series of P3HT/PC70BM PSCs with CuO, Au and ZnO nanoparticles were prepared and analyzed under the same operating conditions. A conductive grade poly(3,4-ethylenedioxy-thiophene)-poly(styrenesulfonate) (PEDOT:PSS), 1.3 wt%, was purchased from Sigma-Aldrich and diluted by adding equal volume of H<sub>2</sub>O. Regioregular P3HT Rieke 'E' was purchased from Rieke Metals, Inc., and used as received. PC70BM was purchased from SES Research Inc. and used as received. ITO coated glass slides measuring 25 x 75 x 1.1 mm (10 Ohm/sq., and ITO thickness 20-100nm) were purchased from nanocs.com. CuO NPs in the size range of 10~30 nm, Au NPs with 18nm diameter and nanoparticles of ZnO (18nm diameter) were purchased from nanocs.com.

### 2.2 Device Fabrication

Polymer solar cells containing CuO, Au and ZnO nanoparticles were fabricated in a clean room inside a glove box in an inert atmosphere using nitrogen gas. Three different series of devices were fabricated in this study as described below. A P3HT/PCBM/ CuO NPs hybrid solution was prepared in a two-step process. The first step was to obtain the P3HT/PC70BM blend by dissolving 10 mg of regioregular P3HT and 10 mg of PC70BM in 2 mL chlorobenzene. The mixture was stirred at 50 °C for 12 hours. The second step is the incorporation of CuO NPs into the blend by dispersing CuO NPs in 2ml of chlorobenzene and adding it to the P3HT/PCBM blend in weights leading to the final weight ratios (P3HT/PCBM/CuO-NPs) of 10:10:0.2; 10:10:0.4; 10:10:0.6; 10:10:0.8; and 10:10:1 mg; respectively. The devices were fabricated in a glove box in nitrogen atmosphere by depositing layers of the materials on a 1 mm glass substrate. The transparent electrode ITO (Merck) was ultrasonically cleaned using a series of solvents like ammonia/hydrogen peroxide/deionized water mixture, methanol, and isopropyl alcohol. The PEDOT/PSS layer with a thickness of 40 nm was spin coated at 4000 rpm on the substrate and then baked at 120 °C for 15 minutes. This serves as a thin hole-transport layer.

Once the sample is cooled to room temperature, the hybrid solution containing P3HT/PC70BM/CuO NPs was deposited by spin-coating at 800 rpm for one minute, which leads to a film thickness of about 100-150 nm. The purpose of this layer is to serve as the active layer. The upper cathode layer with a thickness of approximately 100nm was formed by thermally evaporating Aluminum under high vacuum.

The final device had an area of 0.12 cm<sup>2</sup>. A schematic illustration of the structure of the photovoltaic devices which are fabricated for this study is shown in Figure 1(a).

The second series of devices was fabricated by incorporating Au NPs in the PEDOT:PSS hole transport layer of the first series of devices. In this phase, different amounts of Au NPs were added to 10 ml of PEDOT:PSS aqueous solution, leading to six PEDOT:PSS solutions with 0, 0.02, 0.06, 0.10, 0.14, and 0.18 mg of NPs; respectively. The P3HT/PCBM active layer contained 0.6mg of CuO NPs. The solar cell device structure that was spun coated in this stage is schematically presented in Figure 1(b).

The third series of devices was fabricated by adding an electron transport buffer layer on top of the P3HT/PCBM/0.6 mg CuO-NPs active layer. To prepare ZnO NPs solution, different amounts of ZnO nanoparticles were dispersed in pure ethanol to make four solutions with concentrations of 10, 20, 30, and 40 mg ml<sup>-1</sup> of NPs. The ZnO NPs solution was spin coated for two minutes at 1000 rpm on the above mentioned active layer. In this study, five different devices (reference cell, 10, 20, 30 and 40 mg ml<sup>-1</sup> ZnO NPs in the buffer layer) were fabricated. The active layers measured 120 nm in average thickness and 0.12 cm<sup>2</sup> in surface area. The ZnO film thickness obtained was approximately 60 nm. The structure of the fabricated solar cell devices is schematically presented in Figure 1(c).

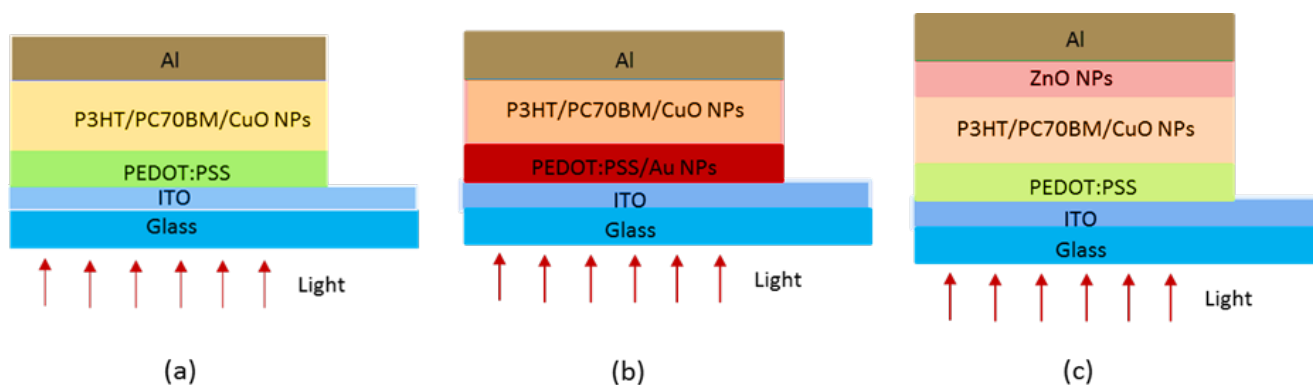


**Figure 1:** Graphical representation of the hybrid device architectures measurements

### 3. Results and discussion

The electrical performance of all hybrid devices containing NPs improved in comparison to their reference devices. This can be attributed to the enhanced optical, morphological and electronic properties of the polymer films with NPs. The short-circuit current density ( $J_{sc}$ ), open-circuit voltage ( $V_{oc}$ ), fill factor ( $FF = \frac{J_m V_m}{J_{sc} V_{oc}}$ ) and power conversion efficiency, which is defined as the ratio of the products of

$V_{oc}$ ,  $J_{sc}$  and FF to the total incident power density ( $PCE = \eta = \frac{J_{sc} V_{oc} FF}{P_{in}}$ ), of all the cells are listed in

Table 1.

Upon adding CuO NPs into the P3HT:PC70BM layer,  $J_{sc}$  increased from 5.233 to 6.487 mA/cm<sup>2</sup> and the FF increased from 61.13% to 68.0%, which is an 11.2% improvement in comparison to the cells without CuO NPs. Although the FF increased steadily in all the cells, the maximum  $J_{sc}$  was achieved at 0.6 mg of CuO NPs. Beyond 0.6 mg of CuO NPs, the  $J_{sc}$  starts to decline, while the  $V_{oc}$  does not change significantly. As a result, the PCE follows the same trend, increasing from 2.10% to 2.96% and then decreasing with subsequent increase in the amounts of CuO in the solar cell. In spite of this behavior, the increase in PCE translates to a 24.2% enhancement in the cells containing 0.6 mg of CuO NPs in comparison to the reference cells.

**Table 1.** Summary of electrical performance parameters: (a) P3HT/PCBM/CuO-NPs, (b) PEDOT:PSS (with Au-NPs)/P3HT/PCBM/CuO-0.6mg NPs (c) P3HT/PCBM/CuO-0.6mg NPs/ZnO NPs

(a) P3HT/PCBM/CuO-NPs

<b>CuO NPs (mg)</b>	<b>J<sub>sc</sub> (mA/cm<sup>2</sup>)</b>	<b>V<sub>oc</sub> (V)</b>	<b>FF(%)</b>	<b>PCE(%)</b>
0	5.233	0.658	61.13	2.106
0.2	5.727	0.675	66.52	2.571
0.4	5.992	0.670	66.21	2.632
0.6	6.487	0.673	68.00	2.963
0.8	6.320	0.668	68.50	2.895
1.0	6.122	0.674	66.84	2.758

(b) PEDOT:PSS (with Au-NPs)/P3HT/PCBM/CuO-0.6mg NPs

<b>Au-NPs(mg)</b>	<b>J<sub>sc</sub>(A/cm<sup>2</sup>)</b>	<b>V<sub>oc</sub>(V)</b>	<b>FF(%)</b>	<b>PCE(%)</b>
0	6.487	0.673	68.00	2.963
0.02	7.006	0.678	68.52	3.255
0.06	7.491	0.677	69.21	3.510
0.10	6.901	0.685	67.02	3.168
0.14	5.984	0.671	67.54	2.712
0.18	4.195	0.673	65.91	1.861

(c) P3HT/PCBM/CuO-0.6mg NPs/ZnO NPs

<b>ZnO NPs(mg)</b>	<b>J<sub>sc</sub>(A/cm<sup>2</sup>)</b>	<b>V<sub>oc</sub>(V)</b>	<b>FF(%)</b>	<b>PCE(%)</b>
0	6.480	0.677	68.11	2.988
10	7.063	0.688	71.44	3.472
20	7.620	0.696	74.47	3.950
30	7.437	0.702	72.46	3.784
40	7.379	0.714	69.79	3.677

However, after adding Au-NPs into the PEDOT:PSS layer, J<sub>sc</sub> increased from 6.487 to 7.491 mA/cm<sup>2</sup>; the fill factor (FF) increased from 68 to 69.21%; while V<sub>oc</sub> remained nearly the same. Subsequently, the improved J<sub>sc</sub> and FF enhanced the power conversion efficiency (PCE) from 2.963 to 3.51%. The incorporation of Au-NPs in the PEDOT:PSS layer contributed to about 18% increase in PCE due to the notably enhanced J<sub>sc</sub> and improved FF.

The third series of devices were fabricated by assembling a ZnO NPs buffer layer in the optimum solar cells containing 0.6mg of CuO NPs in the active layer. The electrical performance parameters were further enhanced. The optimum photovoltaic parameters were obtained by the devices with 20mg ZnO NPs in the electron transport layer ( $J_{sc} = 7.620 \text{ mA cm}^{-2}$ ,  $FF = 74.47\%$ ,  $V_{oc} = 0.696 \text{ V}$ ,  $PCE = 3.950\%$ ). However, the PCE of the solar cells decreased as the ZnO NPs content increased further, while the  $V_{oc}$  remained unchanged.

Figures 2 (a), (b) and (c) show the enhancement in power conversion efficiency (PCE) with the incorporation of CuO nanoparticles in the P3HT/PCBM active layer, Au NPs in the PEDOT:PSS layer, and ZnO nanoparticles in a buffer layer on top of the P3HT/PCBM active layer; respectively.

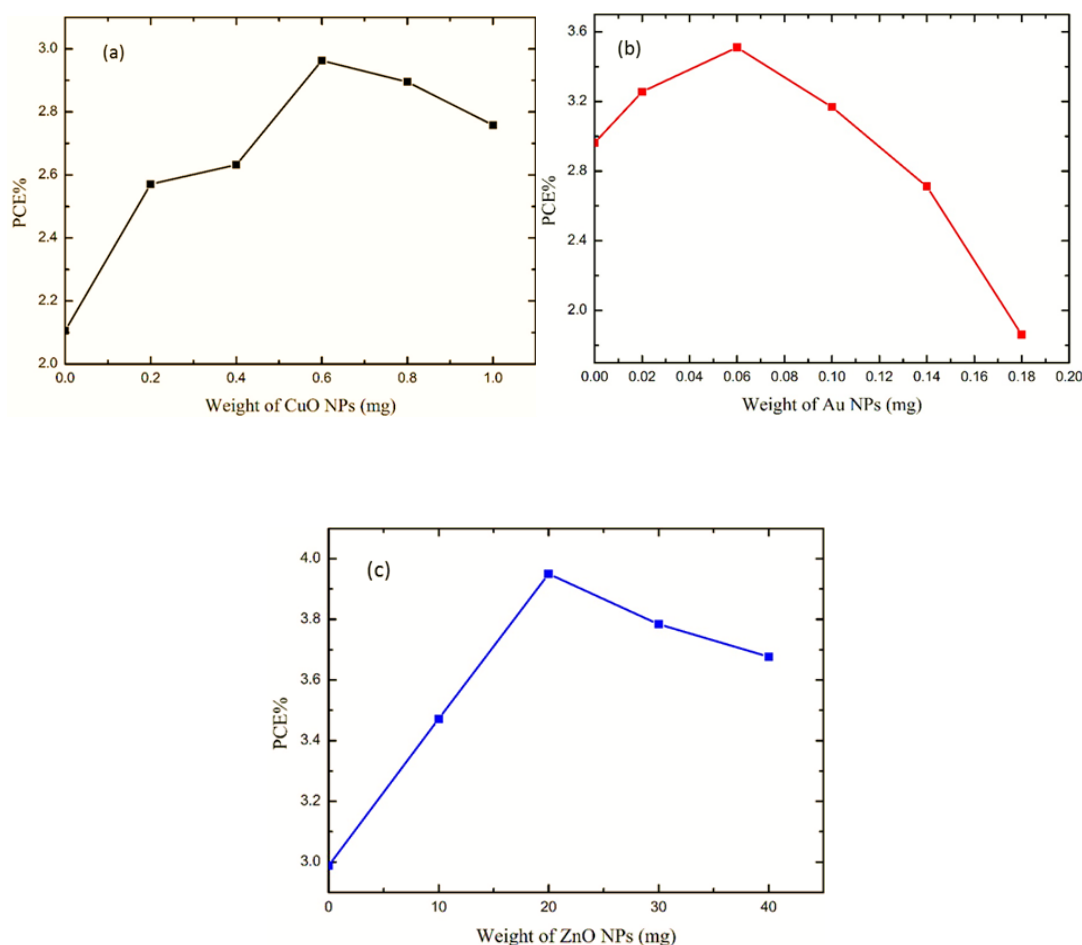


**Figure 2:** PCE of the hybrid solar cells with (a) various CuO NPs concentrations in the P3HT/PCBM active layer (b) various Au NPs concentrations in the PEDOT:PSS layer, (c) various ZnO NPs concentrations in a buffer layer on top of the P3HT/PCBM active layer

The external quantum efficiency (EQE) in solar cells measures the ratio between the incident photons and the generated free charge carriers by the solar cell. EQE spectra of the different sets of solar cells were plotted to better elucidate the observed improvement of  $J_{sc}$  in the fabricated devices. EQE spectra of the devices are shown in Figures 3(a), 3(b) and 3(c). When the nanoparticle densities in the devices were increased, the relevant EQE spectra proportionally enhanced in the wavelength range from 310nm to 650nm. The optimum devices of each series such as CuO, Au and ZnO show highest EQEs of 54.6%, 56.8%, and 57.7%; respectively. The EQE improvements coincide with the  $J_{sc}$  and PCE enhancement of the devices.

The XRD spectrum of the CuO nanoparticles was obtained before incorporating them in the solar cell devices, as shown in Figure 4 (a). The XRD spectra of the P3HT/PC70BM active layers containing various concentrations of CuO NPs is shown in Figure 4 (b). The XRD spectra of the hybrid layers illustrate improved peak intensities over the  $2\theta$  range from  $4.5^\circ$  to  $6^\circ$ , indicating an enhanced crystallinity of the P3HT/PC70BM blend after incorporating CuO NPs.

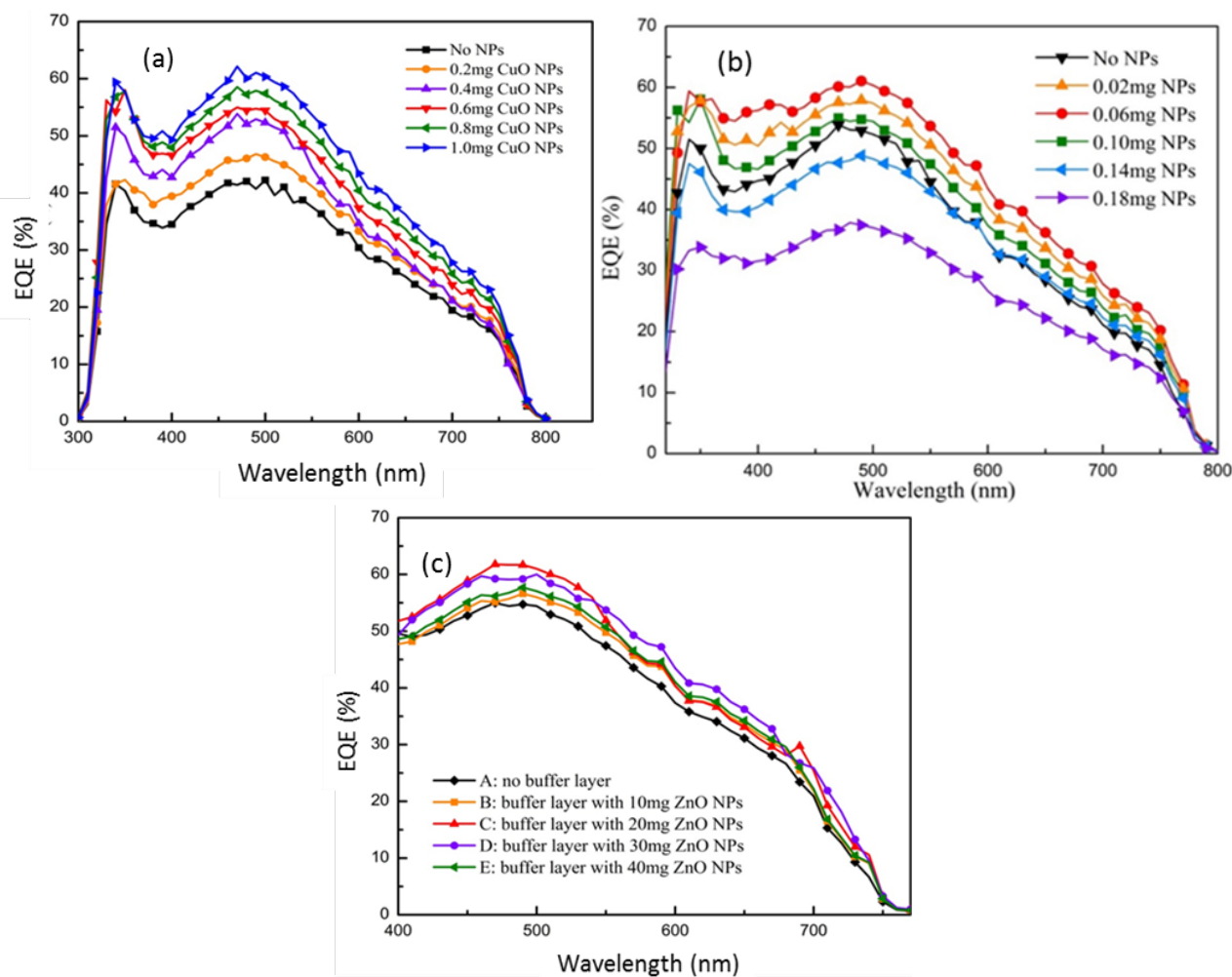


**Figure 3:** EQE of the hybrid solar cells with (a) various CuO NPs concentrations in the P3HT/PCBM active layer (b) various Au NPs concentrations in the PEDOT:PSS layer, (c) various ZnO NPs concentrations in a buffer layer on top of the P3HT/PCBM active layer

The significant increase in P3HT crystallinity, upon adding the CuO NPs, can be ascribed to self-assembly of the conjugated P3HT chains leading to the orderly formation in the blend [31]. In addition, the crystallization of P3HT is faster than the aggregation of PCBM molecules. When the crystallinity of P3HT is enhanced, the crystallization-driven phase separation of P3HT-PCBM will take place. In turn, this increases the PCBM aggregation and the diffusion of PCBM molecules out from the polymer matrix, thus enabling the disordered P3HT to further crystallize. The ordered structure of P3HT leads to enhancing the light absorption and improving the hole mobility [32]. In order to further understand the effect of CuO NPs on the crystallinity of P3HT/PCBM active layers, DSC and XRD spectra were used to calculate the crystallinity of the hybrid active layers as shown in Figure 5. The crystallinity percent, as determined by both XRD and DSC, increases gradually as the amount of CuO NPs increases in the P3HT:PC70BM polymer blend. The CuO NPs encourage the heterogeneous nucleation of P3HT

molecules, which results in an enhanced overall crystallinity. In addition, the increase in crystallinity can be attributed to an improvement in the nanoscale phase-separation of the P3HT/PCBM [33]. The XRD and DSC analysis were carried out for the Au NPs incorporated PEDOT: PSS and bulk ZnO NPs, but no significant peaks were observed for these samples.

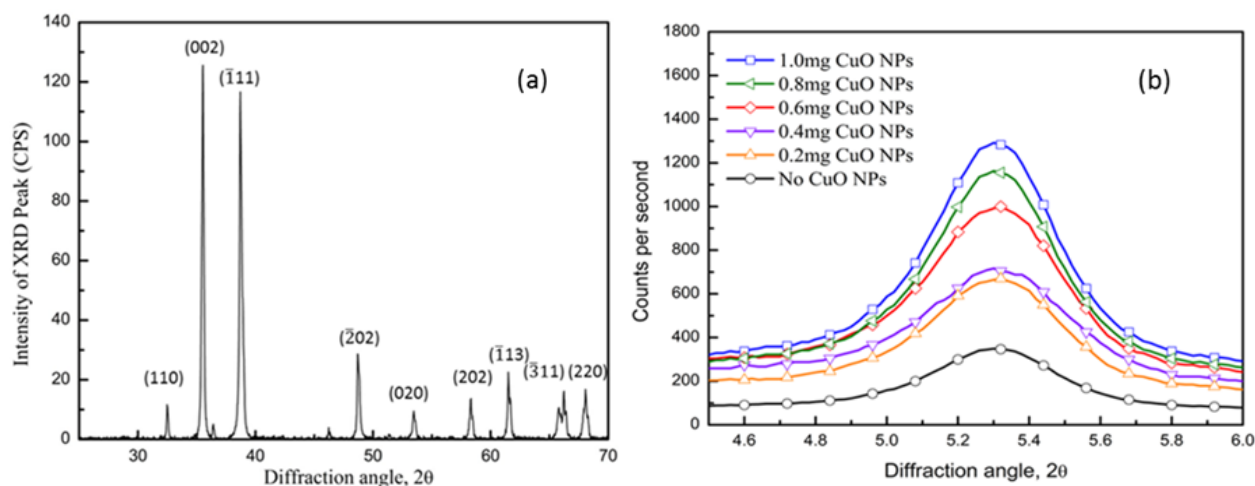


**Figure 4:** XRD spectra (a) CuO NPs (b) P3HT/PCBM-CuO NPs

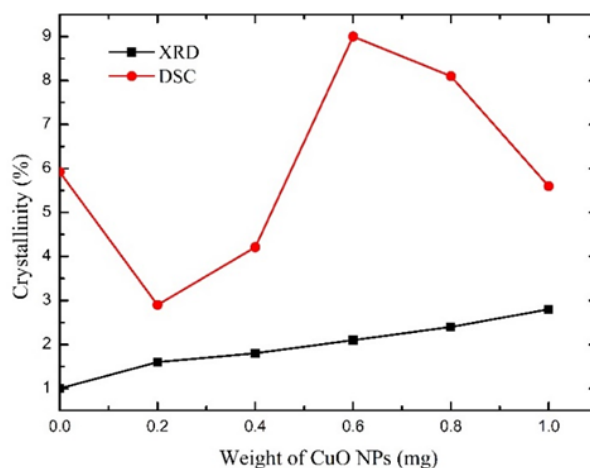


**Figure 5:** Crystallinity % of P3HT/PCBM-CuO NPs hybrid active layers

The spectral diagrams for optical absorption of CuO, Au and ZnO nanoparticle incorporated P3HT/PCBM devices are shown in Figure 6 (a), (b), and (c); respectively. The photon absorption efficiency determines the photon absorption capacity of the solar cells. The light absorption of a semiconductor thin film is controlled by the energy band structure, absorption coefficient, and the thickness of the photoactive layer [34]. According to the spectral diagrams, the optical absorption of P3HT/PCBM solar cells was improved after incorporating CuO and ZnO NPs in the devices. Absorption of a photon with an energy greater than the  $E_g$  value (1.99 eV) for P3HT generates an exciton which is diffused to the P3HT/PCBM interface. The  $E_g$  value of the CuO NPs incorporated P3HT/PCBM was calculated using Tuac formula:  $[(\alpha h\nu)]^m = B(h\nu - E_g)$ . where  $h\nu$  is the energy of the incident photons in eV and  $m = 1/2$  for indirect and 2 for direct allowed transitions,  $B$  is a constant related to the material,  $h$  is Planck's constant,  $\nu$  is the frequency of the photon,  $E_g$  is the optical band gap in eV [35, 36]. Assuming direct transitions between the valence band and the conduction band, the  $E_g$  can be determined by a plot of  $[(\alpha h\nu)]^2$  versus  $(h\nu)$  at  $\alpha=0$ . The estimated  $E_g$  value for CuO NPs is approximately 2.14 eV. The

estimated  $E_g$  value of the P3HT/PCBM blend was 2.71 eV. After incorporating CuO NPs into the P3HT/PCBM blend, the  $E_g$  value was 2.64 eV. However, the  $E_g$  value did not change significantly with changing the concentration of CuO NPs in the blend.

Au NPs improve the light absorption of the thin films due to the localized surface plasmon resonance (LSPR) which contributes to the significant enhancement of local electromagnetic fields which improves the optical properties of the nanostructure devices. The UV-vis absorption measurements of the solar cells, with and without Au-NPs in the PEDOT:PSS layer, did not improve significantly as shown in Figure 6 (b). This can be due to the strong near field surrounding the Au NPs which is distributed horizontally through the PEDOT:PSS thin film, instead of penetrating into the P3HT/PC70BM layer, thus leading to a lower optical absorption. Electrical effects, instead of plasmonic effects, play a major role in the solar cell performance in these devices.

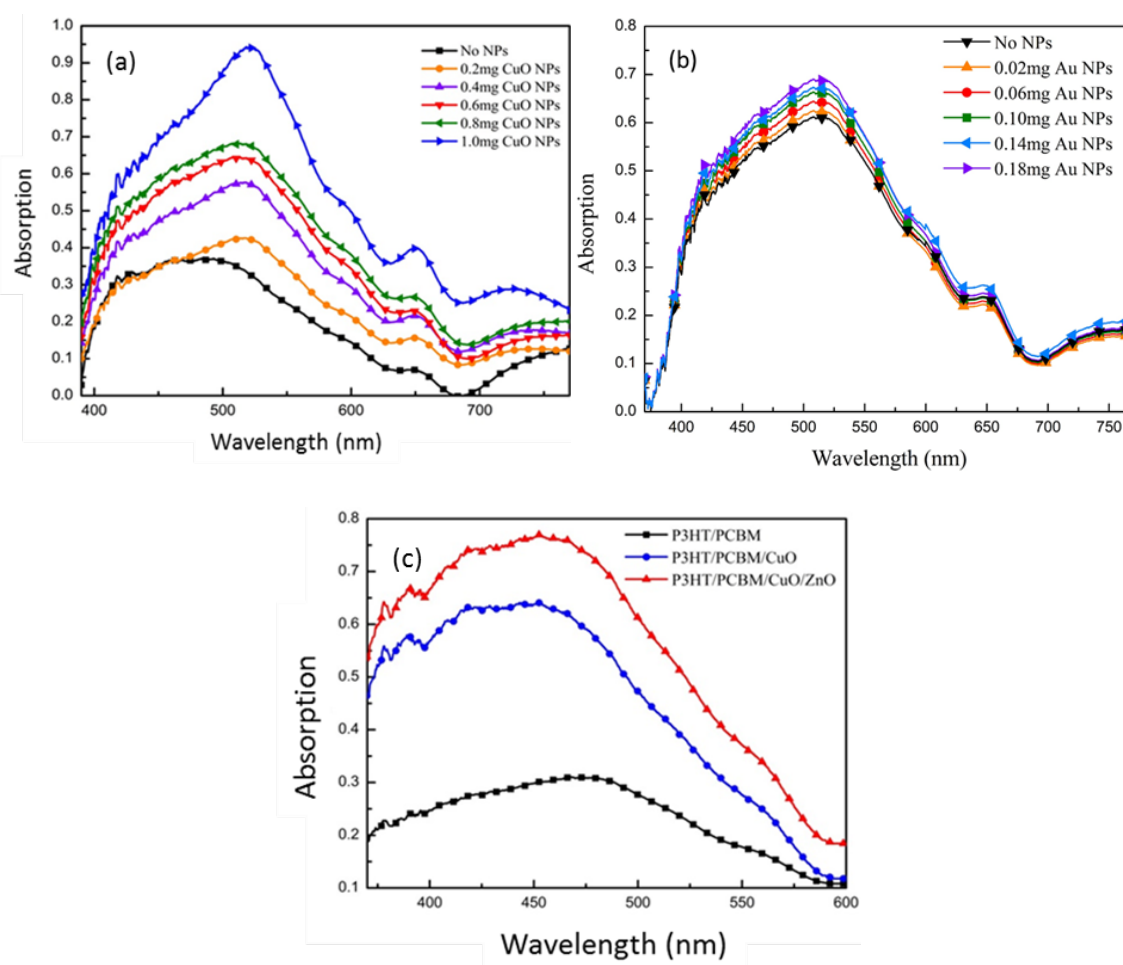


**Figure 6:** Optical absorption spectra: (a) hybrid solar cells with various CuO NPs concentrations in P3HT/PCBM layer (b) various Au NP concentrations in PEDOT: PSS layer (c) hybrid solar cells with ZnO buffer layer

Assembling a ZnO hole transport buffer layer on the P3HT/PCBM/0.6mg of CuO NPs solar cells has notably enhanced the UV vis. Absorption. The ZnO electron transport buffer layer provides an extremely high electron transporting facility to the Al electrodes. The ZnO NPs buffer layer not only increases the light absorption capacity, but also improves the electronic properties of the devices by reducing the recombination of charges at the electrode.

The surface morphology of the active layer plays an important role in optimizing the power conversion efficiency. Surface analysis by AFM was used to understand this phenomenon. The root-mean-square

roughness ( $\sigma_{\text{rms}}$ ) increased from 0.11nm in the thin film without CuO NPs up to 0.47nm in the thin film with 1mg of CuO NPs. The optimum cell with 0.6mg of CuO NPs shows a surface roughness value of 0.32nm. The CuO NPs in the active layer enhance the interfacial distribution by increasing the surface area, which leads to an efficient dissociation of excitons into holes and electrons. Similarly, the AFM images of Au-NP incorporated PEDOT:PSS layers showed a clear enhancement in surface roughness. The  $\sigma_{\text{rms}}$  of the reference film was 0.37nm and it increased to 1.26nm in the samples containing 0.18mg of Au NPs. The optimum cell with 0.06mg of Au-NPs showed a surface roughness value of 0.86nm. The assembly of an electron transporting ZnO NPs layer on the active layer increased the roughness of the P3HT/PC70BM/CuO-NPs thin films. The measured  $\sigma_{\text{rms}}$  of the P3HT/PC70BM/CuO layer was 0.32nm and after depositing the ZnO NPs layer on the active layer, the  $\sigma_{\text{rms}}$  value increased to 0.89nm. The Sample of P3HT/PCBM/CuO-0.6mg NPs with 40mg of ZnO NPs exhibited a maximum surface roughness of 0.97nm. The increased anode surface roughness leads to an increase in the interface contact area between the anode and the active layer, and provides shorter routes for holes to travel to the anode.

## Conclusions

In this study, CuO, Au and ZnO NPs were added to P3HT/PC70BM polymer solar cells to improve the power conversion efficiency. The CuO NPs improved the optical absorption, P3HT crystallinity and surface roughness of P3HT/PC70BM active layer which enhanced the exciton generation, exciton diffusion and charge carrier transportation. In the second series of devices, Au-NPs were added at different amounts to the PEDOT:PSS layer of solar cells containing 0.6mg of CuO-NPs in the active layer. Consequently, the surface roughness of the PEDOT:PSS layer and the series resistance of the devices were improved. Also, the Au NPs contributed to improving the charge carrier collection at the anode and charge carrier transportation. In the third series of devices, ZnO nanoparticles were incorporated in an electron transport buffer layer assembled on top of the P3HT/PC70BM/CuO NPs active later. This buffer layer improved the optical absorption and surface roughness at the anode interface. In addition, the ZnO buffer layer increased the electron mobility in the devices, thus reducing the series resistance. Overall, the incorporation of inorganic nanoparticles in the organic solar cell devices enhanced the light absorption, exciton dissociation and electron collection at the cathode, thus contributing to an overall improvement in the power conversion efficiency of the devices.

## References

1. A. P. Wanninayake, S. Gunashekar, S. Li, B. Church, N. Abu-Zahra, CuO Nanoparticles Based Bulk Heterojunction Solar Cells: Investigations on Morphology and Performance, *J. Sol. Energy Eng.* 137 (2015) 031016.
2. Y. Berredjem, A. Boulmouk, N. Bensid, A. Drici, A.E.K Gheid, A. Bouras, J.C.Bernede, Study of the insertion of a metal layer in an organic solar cell, *J. Mater. Environ. Sci.* 2 (S1) (2011) 544-547
3. A. P. Wanninayake, S. Li, B. Church, N. Abu-Zahra. Electrical and optical properties of hybrid polymer solar cells incorporating Au and CuO nanoparticles, *AIMS Materials Science* 3(1) (2015) 35-50
4. A. P. Wanninayake, S. Li, B. Church, N. Abu-Zahra, Effect of ZnO nanoparticles on the power conversion efficiency of organic photovoltaic devices synthesized with CuO nanoparticles, *AIMS Materials Science* 3(3) (2016) 927-937

5. H. Siddiqui, M. R. Parra, P. Pandey, M.S.Qureshia, F. Z. Haque, Utility of copper oxide nanoparticles (CuO-NPs) as efficient electron donor material in bulk-heterojunction solar cells with enhanced power conversion efficiency, *Journal of Science: Advanced Materials and Devices*, 5(1), (2020),104-110
6. W. Ma, C. Yang, X. Gong, K. Lee, A. J. Heeger, Thermally Stable, Efficient Polymer Solar Cells with Nanoscale Control of the Interpenetrating Network Morphology, *Adv. Funct. Mater.* 15 (10) (2005) 1617–1622
7. A. P. Wanninayake, B. Church, N. Abu-Zahra, Annealing Effect On ZnO-NPs Buffer Layer Assembled Organic Solar Cells Synthesized With CuO Nanoparticles, *Advanced Materials Letters*, 8(1) (2017),08-12
8. R. Raja, W.S.Liu, C. Y. Hsiow, S.P. Rwei, W.Y. Chiu, L. Wang, Terthiophene–C60 dyads as donor/acceptor compatibilizers for developing highly stable P3HT/PCBM bulk heterojunction solar cells, *J. Mater. Chem. A*, 3 (2015) 14401-14408
9. K. Jung, H. J. Song, G. Lee, Y. Ko, K.J. Ahn, H. Choi, J. Y. Kim, K. Ha, J. Song, J. K. Lee, C. Lee., M. Choi, Plasmonic Organic Solar Cells Employing Nanobump Assembly via Aerosol-Derived Nanoparticles, *ACS Nano* 8 (2014) 2590-2601
10. C. Deibel, V. Dyakonov, Polymer-Fullerene Bulk Heterojunction Solar Cells, *Rep. Prog. Phys.* 3 (2010) 9
11. S. Gunes,H. Neugebauer., N. S. Sariciftci, Conjugated Polymer-Based Organic Solar Cells, *Chemical Reviews* 107 (2007) 1324-1338
12. H. A. Atwater, A. Polman, Plasmonics for Improved Photovoltaic Devices, *Nature Materials*, 9 (2010) 205-213
13. J. A. Schuller, E. S. Barnard, W. Cai, Y. C. Jun, J. S. White, M. L. Brongersma, Plasmonics for extreme light concentration and manipulation, *Nature Materials* 9 (2010)193-204
14. A. Y. Mahmoud, R. Izquierdo, V. V. Truong, J Gold Nanorods Incorporated Cathode for Better Performance of Polymer Solar Cells, *Nanomater.* 2014 (2014) 464160
15. M. Wright, A. Uddin, Organic-inorganic hybrid solar cells: A comparative review, *Solar Energy Mater. Solar Cells* 107 (2012) 87–111.
16. A. Moliton, J. M. Nunzi How to model the behaviour of organic photovoltaic cells *Polym Int.*, 55 (2006) 583–600.
17. S. Y. Chou, Ding W., Ultrathin, high-efficiency, broad-band, omni-acceptance, organic solar cells enhanced by plasmonic cavity with subwavelength hole array, *Opt. Express* 21 (2013)60-76
18. A. P. Wanninayake, S. Gunashekar, S. Li, B. Church, N. Abu-Zahra, Performance enhancement of polymer solar cells using copper oxide nanoparticles, *Semicond. Sci. Technol.* 30 (2015) 064004.
19. F. X. Xie, W. C. H. Choy, C.C.D.Wang, W.E.I Sha, D.D.S.Fung, Improving the efficiency of polymer solar cells by incorporating gold nanoparticles into all polymer layers, *Appl. Phys. Lett.* 99 (2011) 153304
20. D. H. Wang, D. Y. Kim., K. W. Choi., J. H. Seo., S. H. Im., J. H. Par., O. Park.,A. J. Heeger, Enhancement of Donor–Acceptor Polymer Bulk Heterojunction Solar Cell Power Conversion Efficiencies by Addition of Au Nanoparticles, *Angew. Chem. Int. Ed.* 50 (2011) 5519–5523
21. E.Salima, S.R.Bobbara, A.Orabya, J.M.Nunzi, Copper oxide nanoparticle doped bulk-heterojunction photovoltaic devices, *Synthetic Metals*, 252, (2019), 21-28

22. D. D. S. Fung, L. F. Qiao., W. C. H. Choy, C. Wang., W. E. I Sha, F. Xie, S. He, Optical and electrical properties of efficiency enhanced polymer solar cells with Au nanoparticles in a PEDOT-PSS layer, *J. Mater. Chem.* 21 (2011) 16349–16356.
23. A. P. Wanninayake, S. Li, B. Church, N. Abu-Zahra, Thermal Annealing on P3HT/PC70BM Solar Cells Incorporated with Au and CuO Nanoparticles, *International Journal of Renewable Energy Research*, 5(4), (2015) 1080-1091
24. Y. M. Chang, L. Wang, Efficient poly(3-hexylthiophene)-based bulk heterojunction solar cells fabricated by an annealing-free approach, *J. Phys. Chem. C* 112, (2008) 17716-17720.
25. G.L. Monroy, M.J. Bedzyk, S. Chattopadhyay, Characterization of polystyrene thin films using X-ray reflectivity. *Nanoscope* 8, (2015) 18–21
26. Q. Gan, F. J. Bartoli, Z. H. Kafafi, Plasmonic-Enhanced Organic Photovoltaics: Breaking the 10% Efficiency Barrier, *Adv. Mater.*, 25 (2013) 2385–2396
27. W. C. H. Choy, The emerging multiple metal nanostructures for enhancing the light trapping of thin film organic photovoltaic cells, *Chem. Commun.*, 50 (2014) 11984-11993
28. Y.M. Chang, L. Wang, Efficient poly(3-hexylthiophene)-based bulk heterojunction solar cells fabricated by an annealing-free approach. *J. Phys. Chem. C* 112, (2008) 17716–17720
29. E. Bundgaard, S. E. Shaheen, F. C. Krebs, D. S. Ginley, Bulk heterojunctions based on a low band gap copolymer of thiophene and benzothiadiazole, *Solar Energy Materials and Solar Cells*, 91 (2007) 1631–1637.
30. M. Wright, A. Uddin, Organic-inorganic hybrid solar cells: A comparative review, *Solar Energy Mater. Solar Cells* 107 (2012) 87–111.
31. M. Nasiri, F. Abbasi, Effect of 1,8-diiodooctane on the performance of P3HT:PCBM solar cells. *J. Sol. Energy Eng.* 137, (2015) 034506
32. A. P. Wanninayake, S. Gunashekar, S. Li, B. Church, N. Abu-Zahra, Effect of Thermal Annealing on the Power Conversion Efficiency of CuO-Bulk Heterojunction P3HT/PC70BM Solar Cells, *Journal of Sustainable Energy Engineering* 3(2) (2015) 107-126
33. G. Li, V. Shrotriya, Y. Yao, Y. Yang, Investigation of annealing effects and film thickness dependence of polymer solar cells based on poly(3-hexylthiophene), *J. Appl. Phys.*, 98 (2005) 043704-1
34. K. Kim, D. L. Carroll, Roles of Au and Ag nanoparticles in efficiency enhancement of poly(3-octylthiophene)/C60 bulk heterojunction photovoltaic devices *Appl. Phys. Lett.*, 87 (2005) 203113
35. F. C. Krebs, Y. Thomann, R. Thomann, J. W. Andreasen, A simple nanostructured polymer/ZnO hybrid solar cell-preparation and operation in air, *Nanotechnology* 19 (2008) 424013
36. A.M. El Sayed, S. El-Gamal, W. M. Morsi, G. Mohammed, Effect of PVA and copper oxide nanoparticles on the structural, optical, and electrical properties of carboxymethyl cellulose films, *J Mater Sci.* 50 (2015) 4717–4728.

(2020) ; <http://www.jmaterenvironsci.com>